

Time-dependent exchange-correlation hole and potential of the electron gas

K. Karlsson¹ and F. Aryasetiawan²

¹*Department of Engineering Sciences, University of Skövde, SE-541 28 Skövde, Sweden*

²*Department of Physics, Division of Mathematical Physics,
Lund University, Professorsgatan 1, 223 63, Lund, Sweden*

The exchange-correlation hole and potential of the homogeneous electron gas have been investigated within the random-phase approximation, employing the plasmon-pole approximation for the linear density response function. The angular dependence as well as the time dependence of the exchange-correlation hole are illustrated for a Wigner-Seitz radius $r_s = 4$ (atomic unit). It is found that there is a substantial cancellation between exchange and correlation potentials in space and time, analogous to the cancellation of exchange and correlation self-energies. Analysis of the sum rule explains why it is more advantageous to use a non-interacting Green function than a renormalized one when calculating the response function within the random-phase approximation and consequently the self-energy within the well-established *GW* approximation. The present study provides a starting point for more accurate and comprehensive calculations of the exchange-correlation hole and potential of the electron gas with the aim of constructing a model based on the local density approximation as in density functional theory.

I. INTRODUCTION

The homogeneous electron gas has been a long-lasting and an invaluable model of valence electrons in solids. Pseudopotential theory¹ explains why the behavior of valence electrons in solids, despite the presence of a strong ionic potential, nevertheless resembles that of the electron gas. The effects of exchange and correlations of the interacting homogeneous electron gas have been studied thoroughly for the last six decades²⁻⁴. An important empirical observation is that the main features of the spectral function arising from exchange and correlations are quite robust and can be carried over to real materials. For example, setting aside strongly correlated systems⁵, it is generally the case that the spectral function of most materials consists of a quasiparticle peak and an incoherent satellite feature which can be traced back to collective charge excitations (plasmons), just as found in the electron gas⁶.

The effects of exchange and correlations have been traditionally studied using the concept of self-energy, a non-local and energy-dependent quantity that acts on the Green function as a convolution in space and time^{7,8}. In a recent development, a different framework for representing exchange and correlations was proposed in the form of a time-dependent exchange-correlation (xc) potential^{9,10}. This formalism is fundamentally different from the self-energy approach in that the potential acts locally or multiplicatively on the Green function. Most importantly, the potential arises naturally as a Coulomb potential of a charge distribution (exchange-correlation hole) which fulfills a sum rule and some exact properties. Moreover, due to the special form of the Coulomb interaction, which depends solely on the separation of two point charges, it can be shown that the exchange-correlation potential is in fact the first radial moment of the spherical average of the exchange-correlation hole. This appealing result is the analog of the result found in the exact expression for the ground-state exchange-correlation

energy, which is very much utilized in density functional theory and partially explains the success of the local density approximation^{11,12}.

The exchange-correlation potential formalism also provides a simple physical picture of the propagation of an added hole or electron in a many-electron system as in photoemission and inverse photoemission experiments. The added hole or electron induces a temporal density fluctuation of the system initially in its ground state, giving rise to the exchange-correlation potential, which in turn acts on the Green function representing the propagation of the added hole or electron.

In this paper, the time-dependent exchange-correlation hole and its corresponding exchange-correlation potential of the electron gas are studied using the random-phase approximation (RPA)^{3,7,13} to understand the salient features of the exchange-correlation hole and potential. The long-term goal is to use the electron gas results as a basis for a local density approximation in the spirit of density functional theory^{12,14-17}.

The theory section commences with a short summary of the exchange-correlation potential framework, which is outlined in detail in previous publications. Formulas for the exchange-correlation hole and potential are then derived for the homogeneous electron gas. An analysis of the sum rule and its consequences is presented in Sec. II F followed by computational results in Sec. III and a summary at the end.

II. THEORY

In the exchange-correlation potential formalism the equation of motion of the equilibrium zero temperature time-ordered Green function is given by⁹

$$\left(i \frac{\partial}{\partial t} - h(r) - V_{xc}(r, r'; t) \right) G(r, r'; t) = \delta(r - r') \delta(t), \quad (1)$$

where

$$h(r) = -\frac{1}{2}\nabla^2 + V_{\text{ext}}(r) + V_{\text{H}}(r), \quad (2)$$

in which V_{ext} and V_{H} are the external field and the Hartree potential, respectively. The Green function is defined according to⁷

$$iG(r, r'; t) = \langle T[\hat{\psi}(rt)\hat{\psi}^\dagger(r'0)] \rangle, \quad (3)$$

where $r = (\mathbf{r}, \sigma)$ labels both space and spin variables, $\hat{\psi}(rt)$ is the Heisenberg field operator, T is the time-ordering symbol, and $\langle \cdot \rangle$ denotes expectation value in the ground state.

The exchange-correlation potential V_{xc} is the Coulomb potential of the exchange-correlation hole ρ_{xc} :

$$V_{\text{xc}}(r, r'; t) = \int dr'' v(r - r'') \rho_{\text{xc}}(r, r', r''; t). \quad (4)$$

The presence of the instantaneous Coulomb interaction implies that $t'' = t$. The exchange-correlation hole fulfills an important sum rule

$$\int d^3r'' \rho_{\text{xc}}(r, r', r''; t) = -\delta_{\sigma\sigma'} \theta(-t) \quad (5)$$

and the following exact condition

$$\rho_{\text{xc}}(r, r', r'' = r; t) = -\rho(r) \quad (6)$$

for any r, r' and t .

A. General formula for the exchange-correlation hole

From the definition of the exchange-correlation hole⁹,

$$\begin{aligned} G^{(2)} &= \langle T[\hat{\rho}(3)\hat{\psi}(1)\hat{\psi}^\dagger(2)] \rangle \\ &= i[\rho(3) + \rho_{\text{xc}}(1, 2, 3)]G(1, 2), \end{aligned} \quad (7)$$

where $1 = (r_1, t_1)$ etc. with $t_1 = t_3$ and the relation^{2,6}

$$G^{(2)} = i\rho(3)G(1, 2) - \frac{\delta G(1, 2)}{\delta\varphi(3)}, \quad (8)$$

an explicit formula for the exchange-correlation hole is given by¹⁰

$$\rho_{\text{xc}}(1, 2, 3) = i \frac{\delta}{\delta\varphi(3)} \ln G(1, 2), \quad (9)$$

where φ is a probing field, which is set to zero after the functional derivative is taken. The exchange-correlation hole can thus be regarded as the linear response of $i \ln G$ with respect to an external field.

From the identity

$$\delta G = -G(\delta G^{-1})G \quad (10)$$

and the equation of motion of the Green function, one obtains

$$\begin{aligned} &\rho_{\text{xc}}(1, 2, 3)G(1, 2) \\ &= i \int d4 G(1, 4) \left\{ \delta(3 - 4) + \frac{\delta V_{\text{H}}(4)}{\delta\varphi(3)} \right\} G(4, 2) \\ &+ i \int d4d5 G(1, 4) \frac{\delta\Sigma(4, 5)}{\delta\varphi(3)} G(5, 2), \end{aligned} \quad (11)$$

where Σ is the self-energy. The first term on the right-hand side, $iG(1, 3)G(3, 2)$, will be referred to as the exchange contribution, the second term involving $\frac{\delta V_{\text{H}}}{\delta\varphi}$ as the linear response contribution, and the last term with $\frac{\delta\Sigma}{\delta\varphi}$ as the vertex correction. The second and third terms together constitute the correlation contribution. Within the RPA, the vertex correction is neglected.

The quantity in the curly brackets is the inverse dielectric function:

$$\epsilon^{-1}(4, 3) = \delta(4 - 3) + \frac{\delta V_{\text{H}}(4)}{\delta\varphi(3)}. \quad (12)$$

It is convenient for later purposes to define

$$K(4, 3) = \frac{\delta V_{\text{H}}(4)}{\delta\varphi(3)} = \int d5 v(4 - 5)\chi(5, 3), \quad (13)$$

where v is the Coulomb interaction and χ is the linear density response function

$$\chi(5, 3) = \frac{\delta\rho(5)}{\delta\varphi(3)}. \quad (14)$$

Replacing $r_1 \rightarrow r$, $r_2 \rightarrow r'$, and $r_3 \rightarrow r''$ and taking into account the fact that $t_1 = t_3 = t$ and $t_2 = 0$, one finds

$$\begin{aligned} &\rho_{\text{xc}}(r, r', r''; t)G(r, r'; t) = iG(r, r''; 0^-)G(r'', r'; t) \\ &+ i \int dr_4 dt_4 G(r, r_4; t - t_4)K(r_4, r''; t_4 - t)G(r_4, r'; t_4). \end{aligned} \quad (15)$$

The first term on the right-hand side yields the exchange hole whereas the second term yields the correlation hole. It is immediately clear that the exact condition in Eq. (6) is already fulfilled by the exchange hole implying that

$$\rho_{\text{c}}(r, r', r; t) = 0. \quad (16)$$

B. Interacting homogeneous electron gas

The Green function of the paramagnetic non-interacting homogeneous electron gas is given by

$$\begin{aligned} iG_0(r, r'; t) &= \frac{1}{\Omega} \sum_{k > k_{\text{F}}} e^{i\mathbf{k}\cdot(\mathbf{r}-\mathbf{r}')} e^{-i\varepsilon_k t} \theta(t) \\ &- \frac{1}{\Omega} \sum_{k \leq k_{\text{F}}} e^{i\mathbf{k}\cdot(\mathbf{r}-\mathbf{r}')} e^{-i\varepsilon_k t} \theta(-t), \end{aligned} \quad (17)$$

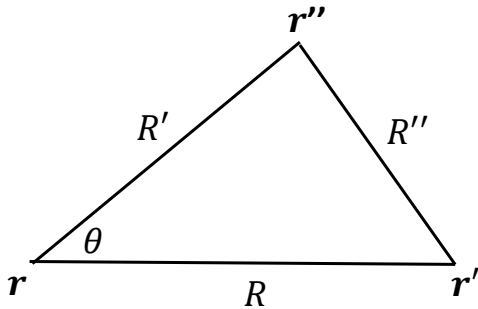


FIG. 1: Definition of the radial variables R , R' , and R'' . They are related to the angle θ by $R''^2 = R^2 - 2RR' \cos \theta + R'^2$

where $\varepsilon_k = \frac{1}{2}k^2$, k_F is the Fermi wave vector, and Ω is the space volume. It is understood that $\sigma = \sigma'$. For the homogeneous electron gas, it is convenient to introduce the variable $\mathbf{R} = \mathbf{r}' - \mathbf{r}$. In spherical coordinates the equation of motion becomes

$$\left(i \frac{\partial}{\partial t} - h(R) - V_{xc}(R; t) \right) \tilde{G}(R, t) = \frac{1}{4\pi R} \delta(R) \delta(t), \quad (18)$$

where

$$h(R) = -\frac{1}{2} \frac{\partial^2}{\partial R^2}, \quad \tilde{G}(R, t) = R G(R, t). \quad (19)$$

Defining

$$T(R, t) = \frac{1}{\tilde{G}(R, t)} h(R) \tilde{G}(R, t), \quad (20)$$

the formal solution is given by

$$G(R, t) = G(R, 0) e^{-i \int_0^t dt' [T(R, t') + V_{xc}(R, t')]}, \quad (21)$$

in which it is understood that $G(R, 0) = G(R, 0^+)$ for $t > 0$ and $G(R, 0) = G(R, 0^-)$ for $t < 0$. In general, from the equation of motion in Eq. (18)

$$i[G(R, 0^+) - G(R, 0^-)] = \frac{\delta(R)}{4\pi R^2}. \quad (22)$$

For the homogeneous electron gas, \mathbf{r} may be chosen to be the origin, i.e., $\mathbf{r} = 0$, and one defines the variables $\mathbf{R} = \mathbf{r}' - \mathbf{r}$, $\mathbf{R}' = \mathbf{r}'' - \mathbf{r}$, and $\mathbf{R}'' = \mathbf{r}'' - \mathbf{r}'$ as illustrated in Fig. 1.

C. Exchange hole

From Eq. (15) the exchange hole is given by

$$\rho_x(r, r', r''; t) G(r, r'; t) = iG(r, r''; 0^-) G(r'', r'; t). \quad (23)$$

Unlike the static exchange hole¹⁸ in quantum chemistry and density functional theory, the exchange hole in the present formalism is time dependent.

Using a non-interacting Green function as given in Eq. (17) and considering the case $t < 0$ one finds

$$\begin{aligned} \rho_x(r, r', r''; t < 0) & \sum_{k \leq k_F} e^{i\mathbf{k} \cdot (\mathbf{r} - \mathbf{r}')} e^{-i\varepsilon_k t} \\ & = -\frac{1}{\Omega} \sum_{k' \leq k_F} e^{i\mathbf{k}' \cdot (\mathbf{r} - \mathbf{r}'')} \times \sum_{k \leq k_F} e^{i\mathbf{k} \cdot (\mathbf{r}'' - \mathbf{r}')} e^{-i\varepsilon_k t}. \end{aligned} \quad (24)$$

For $t > 0$

$$\begin{aligned} \rho_x(r, r', r''; t > 0) & \sum_{k > k_F} e^{i\mathbf{k} \cdot (\mathbf{r} - \mathbf{r}')} e^{-i\varepsilon_k t} \\ & = -\frac{1}{\Omega} \sum_{k' \leq k_F} e^{i\mathbf{k}' \cdot (\mathbf{r} - \mathbf{r}'')} \times \sum_{k > k_F} e^{i\mathbf{k} \cdot (\mathbf{r}'' - \mathbf{r}')} e^{-i\varepsilon_k t}. \end{aligned} \quad (25)$$

Expressed in radial variables and the angle θ as explained in Fig. 1,

$$\rho_x(R, R', \theta; t) = iG_0(R', 0^-) \frac{G_0(R'', t)}{G_0(R, t)} \quad (26)$$

where R'' depends on θ .

$G_0(R, t)$ is obtained from Eq. (17) by performing the \mathbf{k} -integral over the solid angle, yielding

$$iG_0(R, t < 0) = -\frac{1}{2\pi^2} \frac{1}{R} \int_0^{k_F} dk k \sin(kR) e^{-ik^2 t/2}, \quad (27)$$

$$iG_0(R, t > 0) = \frac{1}{2\pi^2} \frac{1}{R} \int_{k_F}^{\infty} dk k \sin(kR) e^{-ik^2 t/2}, \quad (28)$$

$$iG_0(R, 0^-) = -\frac{1}{2\pi^2} \frac{1}{R^3} [\sin(k_F R) - k_F R \cos(k_F R)]. \quad (29)$$

$G_0(R, t < 0)$ can be expressed in terms of the complex error function or calculated numerically using a standard quadrature. The calculation of $G_0(R, t > 0)$, however, needs more care and it is detailed in Appendix A.

D. Correlation hole

The linear response contribution to ρ_{xc} is given by the second term in Eq. (15). Keeping in mind that $t_3 = t_1 = t$, $t_2 = 0$, one obtains

$$\begin{aligned} & i \int d4 G(1, 4) K(4, 3) G(4, 2) \\ & = i \int dr_4 dt_4 G(r - r_4, t - t_4) K(r_4 - r'', t_4 - t) \\ & \quad \times G(r_4 - r', t_4). \end{aligned} \quad (30)$$

The details of the calculations using $G = G_0$ are shown in Appendix B and the results are given by

$$\rho_c(R, R', \theta; t < 0) = \frac{A_1 + A_2}{G_0(R, t < 0)}, \quad (31)$$

$$\rho_c(R, R', \theta; t > 0) = \frac{B_1 + B_2}{G_0(R, t > 0)}. \quad (32)$$

$A_1, A_2, B_1,$ and B_2 are functions of R' and R'' , and given by

$$A_1 = \gamma(R', R'', t, 0, t), \quad (33)$$

$$A_2 = \gamma(R'', R', t, 0, 0), \quad (34)$$

$$B_1 = \gamma(R', R'', 0, t, 0), \quad (35)$$

$$B_2 = \gamma(R'', R', 0, t, -t), \quad (36)$$

where

$$\begin{aligned} \gamma(R, R', t, t', t'') &= \frac{1}{\Omega^2} \sum_{k \leq k_F} e^{-i\mathbf{k} \cdot \mathbf{R}} e^{-i\varepsilon_k t} \\ &\times \sum_{k' > k_F} e^{i\mathbf{k}' \cdot \mathbf{R}'} e^{-i\varepsilon_{k'} t'} M(|\mathbf{k}' - \mathbf{k}|, \varepsilon_{k'} - \varepsilon_k, t''). \end{aligned} \quad (37)$$

The quantity M is given by

$$M(q, \omega, t) = \int_0^\infty d\omega' L(q, \omega') \frac{-ie^{i\omega' t}}{\omega' + \omega}, \quad (38)$$

where $L(q, \omega)$ is the spectral function of $K(q, \omega)$ defined in Eq. (13):

$$K(k, \omega) = \int_{-\infty}^0 d\omega' \frac{L(k, \omega')}{\omega - \omega' - i\delta} + \int_0^\infty d\omega' \frac{L(k, \omega')}{\omega - \omega' + i\delta}. \quad (39)$$

$K(q, \omega)$ is symmetric in frequency but $L(q, \omega)$ is anti-symmetric and related to K as follows:

$$L(k, \omega) = -\frac{1}{\pi} \text{sign}(\omega) \text{Im}K(k, \omega). \quad (40)$$

The correlation hole involves coupled integrals over momenta below and above k_F , which are difficult to calculate analytically. They are six-dimensional integrals which cannot be easily performed with standard quadratures. To make the computation feasible, a plasmon-pole approximation for $L(k, \omega)$ is employed and described in the next section.

1. Plasmon-pole approximation

The plasmon dispersion of the homogeneous electron gas is given by⁷

$$\Omega_q = \omega_p \left(1 + \frac{3}{10} \frac{k_F^2 q^2}{\omega_p^2} + \dots \right), \quad (41)$$

where the plasmon frequency ω_p in the long-wavelength limit is given by

$$\omega_p^2 = 4\pi\rho_0, \quad (42)$$

and ρ_0 is the electron gas density. The critical momentum, q_c , at which the plasmon starts to merge into the electron-hole excitations is given by the crossing of the plasmon dispersion with the line $\varepsilon_q + k_F q$ yielding

$$q_c = \frac{1}{2a} (\sqrt{1 + 4ac} - 1) k_F, \quad (43)$$

where

$$a = \frac{1}{2} - \frac{3}{10c}, \quad c = \frac{\omega_p}{k_F^2}. \quad (44)$$

Great simplification results if a plasmon-pole approximation independent of k is used for $L(k, \omega)$ defined in Eq. (40):

$$L(k, \omega) = \frac{\omega_p}{2} [\delta(\omega - \omega_p) - \delta(\omega + \omega_p)], \quad (45)$$

which corresponds to

$$K(q \rightarrow 0, \omega) = \frac{\omega_p^2}{\omega^2 - \omega_p^2}. \quad (46)$$

The approximation is valid for $k \leq q_c$ and for $r_s = 3, 4$ and 5, which cover most of the average valence densities in real materials, the critical momenta are $q_c = 0.86, 0.82,$ and $0.73 k_F$, respectively.

Within the plasmon-pole approximation the quantity M defined in Eq. (38) becomes independent of momenta:

$$M(q, \omega, t) = \frac{\omega_p}{2} \frac{-ie^{i\omega_p t}}{\omega_p + \omega}. \quad (47)$$

Then the coupling between \mathbf{k} and \mathbf{k}' is partially released. Using

$$\frac{1}{\Omega} \sum_{\mathbf{k}} e^{-i\mathbf{k} \cdot \mathbf{R}} = \frac{1}{2\pi^2 R} \int dk k \sin(kR) \quad (48)$$

yields within the plasmon-pole approximation

$$\begin{aligned} \gamma^{PP}(R, R', t, t', t'') &= \frac{-2i\omega_p}{(2\pi)^4 R R'} \int_0^{k_F} dk k \sin(kR) e^{-i\varepsilon_k t} \\ &\times \int_{k_F}^\infty dk' k' \sin(k'R') \frac{e^{-i\varepsilon_{k'} t'} e^{i\omega_p t''}}{\omega_p + \varepsilon_{k'} - \varepsilon_k}. \end{aligned} \quad (49)$$

Since the plasmon-pole approximation decouples the angular inter-dependence of \mathbf{k} and \mathbf{k}' , it is expected to impart error to the correlation contribution. To minimize error, the upper limit of the integration over k' corresponding to unoccupied states is chosen so as to approximately reproduce the static correlation hole¹⁹. This choice yields a value of $\approx 1.5k_F$ so that integration over unoccupied states arising from the correlation contribution is restricted to between k_F and $1.5k_F$.

E. Exchange-correlation potential

By making a change of variable $\mathbf{R}' = \mathbf{r}'' - \mathbf{r}$ the exchange-correlation potential in Eq. (4) reduces to the first radial moment of the spherical average of ρ_{xc} :

$$V_{xc}(r, r'; t) = \int dR' R' \bar{\rho}_{xc}(r, r', R'; t), \quad (50)$$

where $\bar{\rho}_{xc}(r, r', R'; t)$ for given r, r' , and t depends only on the radial distance $R' = |\mathbf{r}'' - \mathbf{r}|$,

$$\bar{\rho}_{xc}(r, r', R'; t) = \int d\Omega_{R'} \rho_{xc}(r, r', \mathbf{r} + \mathbf{R}'; t). \quad (51)$$

As can be seen from, e.g., Eqs. (24) and (B5), the spherical average of ρ_{xc} for the electron gas amounts to performing a solid-angle integration

$$\int d\Omega'' e^{i(\mathbf{k}-\mathbf{k}') \cdot \mathbf{r}''} = 4\pi \frac{\sin(\Delta k R')}{\Delta k R'}, \quad (52)$$

where $\Delta k = |\mathbf{k} - \mathbf{k}'|$ and $R' = |\mathbf{r}'' - \mathbf{r}|$, $\mathbf{r} = 0$.

1. Exchange potential

For $t < 0$ the exchange hole is given by

$$\begin{aligned} & \bar{\rho}_x(R, R', t < 0) iG_0(R, t) \\ &= \frac{1}{\Omega^2} \sum_{k, k' \leq k_F} e^{-i\mathbf{k} \cdot \mathbf{r}'} e^{-i\varepsilon_k t} \times 4\pi \frac{\sin(\Delta k R')}{\Delta k R'}. \end{aligned} \quad (53)$$

The exchange potential is the first moment of $\bar{\rho}_x$ in R' :

$$\begin{aligned} V_x(R, t < 0) &= \frac{1}{iG_0(R, t) \Omega^2} \sum_{k, k' \leq k_F} e^{-i\mathbf{k} \cdot \mathbf{R}} e^{-i\varepsilon_k t} \\ &\times \int dR' \frac{\sin(\Delta k R')}{\Delta k}. \end{aligned} \quad (54)$$

Consider the integral over R' with positive $\alpha \rightarrow 0$:

$$\lim_{\alpha \rightarrow 0} \int_0^\infty dR' \sin(\Delta k R') e^{-\alpha R'} = \frac{1}{\Delta k}. \quad (55)$$

One then finds

$$V_x(R, t < 0) = \frac{1}{iG_0(R, t) \Omega^2} \sum_{k, k' \leq k_F} e^{-i\mathbf{k} \cdot \mathbf{R}} e^{-i\varepsilon_k t} \frac{1}{(\Delta k)^2}. \quad (56)$$

The integral over k' is given by

$$\begin{aligned} f(k) &= \frac{1}{\Omega} \sum_{k' \leq k_F} \frac{1}{(\Delta k)^2} \\ &= \frac{1}{4\pi^2 k} \int_0^{k_F} dk' k' \ln \left| \frac{k+k'}{k-k'} \right|, \end{aligned} \quad (57)$$

which can be performed analytically yielding

$$f(k) = \frac{k_F}{2\pi^2} F(k/k_F), \quad (58)$$

where

$$F(x) = \frac{1}{2} + \frac{1-x^2}{4x} \ln \left| \frac{1+x}{1-x} \right|. \quad (59)$$

This function is the same as the one appearing in the static Hartree-Fock theory for the electron gas²⁰. More explicitly as a function of k ,

$$f(k) = \frac{k_F}{2\pi^2} \left(\frac{1}{2} + \frac{k_F^2 - k^2}{4k_F k} \ln \left| \frac{k_F + k}{k_F - k} \right| \right). \quad (60)$$

There remains the integral over \mathbf{k} which reduces to a one-dimensional integral over the radial k :

$$\begin{aligned} V_x(R, t < 0) &= \frac{1}{iG_0(R, t)} \\ &\times \frac{2}{\pi R} \int_0^{k_F} dk k \sin(kR) e^{-i\varepsilon_k t} f(k). \end{aligned} \quad (61)$$

For $t > 0$ the result is given by

$$\begin{aligned} V_x(R, t > 0) &= -\frac{1}{iG_0(R, t)} \\ &\times \frac{2}{\pi R} \int_{k_F}^\infty dk k \sin(kR) e^{-i\varepsilon_k t} f(k). \end{aligned} \quad (62)$$

2. Correlation potential

A similar procedure as for the exchange potential can be applied to the correlation potential using A_1, A_2, B_1 , and B_2 , given in Eqs. (B18-B21) in Appendix B.

The result is given by

$$V_c(R, t < 0) = \frac{C_1 + C_2}{G_0(R, t < 0)}, \quad (63)$$

$$V_c(R, t > 0) = \frac{D_1 + D_2}{G_0(R, t > 0)}, \quad (64)$$

where

$$C_1 = \Gamma(0, R, t, 0, t), \quad (65)$$

$$C_2 = \Gamma(R, 0, t, 0, 0), \quad (66)$$

$$D_1 = \Gamma(0, R, 0, t, 0), \quad (67)$$

$$D_2 = \Gamma(R, 0, 0, t, -t), \quad (68)$$

and

$$\begin{aligned} \Gamma(R, R', t, t', t'') &= \frac{4\pi}{\Omega^2} \sum_{k \leq k_F} e^{-i\varepsilon_k t} e^{-i\mathbf{k} \cdot \mathbf{R}} \\ &\times \sum_{k' > k_F} e^{-i\mathbf{k}' \cdot \mathbf{R}'} e^{-i\varepsilon_{k'} t'} \times \frac{M(|\mathbf{k}' - \mathbf{k}|, \varepsilon_{k'} - \varepsilon_k, t'')}{|\mathbf{k}' - \mathbf{k}|^2}. \end{aligned} \quad (69)$$

According to Eq. (47), within the plasmon-pole approximation,

$$M(|\mathbf{k}' - \mathbf{k}|, \varepsilon_{k'} - \varepsilon_k, t'') = \frac{\omega_p}{2} \frac{-ie^{i\omega_p t''}}{\omega_p + \varepsilon_{k'} - \varepsilon_k}, \quad (70)$$

which partially decouples the interdependence of \mathbf{k} and \mathbf{k}' , allowing for analytical integration over the solid angles of both variables, yielding

$$C_1 = P_1(R, t, 0, t), \quad (71)$$

$$C_2 = P_2(R, t, 0, 0), \quad (72)$$

$$D_1 = P_1(R, 0, t, 0), \quad (73)$$

$$D_2 = P_2(R, 0, t, -t), \quad (74)$$

where

$$P_1(R, t, t', t'') = \frac{-i\omega_p e^{i\omega_p t''}}{4\pi^3 R} \int_0^{k_F} dk \int_{k_F}^{\infty} dk' k \sin(k'R) \times \frac{e^{-i\varepsilon_k t} e^{-i\varepsilon_{k'} t'}}{\omega_p + \varepsilon_{k'} - \varepsilon_k} \ln \left| \frac{k + k'}{k - k'} \right|, \quad (75)$$

$$P_2(R, t, t', t'') = \frac{-i\omega_p e^{i\omega_p t''}}{4\pi^3 R} \int_0^{k_F} dk \int_{k_F}^{\infty} dk' k' \sin(kR) \times \frac{e^{-i\varepsilon_k t} e^{-i\varepsilon_{k'} t'}}{\omega_p + \varepsilon_{k'} - \varepsilon_k} \ln \left| \frac{k + k'}{k - k'} \right|. \quad (76)$$

Due to the use of the plasmon-pole approximation, the upper limit of the integral over k' is restricted to $1.5k_F$ to reproduce approximately the static correlation hole, as described earlier in Sec. IID 1.

F. Sum rule

In this section, the sum rule and its consequences are discussed and a simple vertex approximation respecting the sum rule is proposed. The results and conclusions reached in this section are quite general and supported by the electron gas results.

1. Exchange hole

One has for a non-interacting G and $t < 0$

$$i \int dr'' G_0(r, r''; 0^-) G_0(r'', r'; t < 0) = -G_0(r, r'; t < 0), \quad (77)$$

which can be shown as follows:

$$\begin{aligned} & i \int dr'' G_0(r, r''; 0^-) G_0(r'', r'; t < 0) \\ &= -i \int dr'' \sum_{k \leq k_F} \varphi_k(r) \varphi_k^*(r'') \sum_{k' \leq k_F} \varphi_{k'}(r'') \varphi_{k'}^*(r') e^{-i\varepsilon_{k'} t} \\ &= -i \sum_{k \leq k_F} \varphi_k(r) \varphi_k^*(r') e^{-i\varepsilon_k t} \\ &= -G_0(r, r'; t < 0). \end{aligned} \quad (78)$$

It is also quite clear that

$$i \int dr'' G_0(r, r''; 0^-) G_0(r'', r'; t > 0) = 0. \quad (79)$$

It then follows from Eq. (23) that the exchange hole fulfills the sum rule when G_0 is used:

$$\int dr'' \rho_x(r, r', r''; t < 0) = -1. \quad (80)$$

Explicitly for the electron gas, it follows from Eq. (24) that the sum rule for $t < 0$ is fulfilled by the exchange hole since

$$\int d^3 r'' e^{i(\mathbf{k} - \mathbf{k}') \cdot \mathbf{r}''} = (2\pi)^3 \delta(\mathbf{k} - \mathbf{k}'). \quad (81)$$

The sum rule for $t > 0$ is zero since $\mathbf{k} \neq \mathbf{k}'$ as can be seen from Eq. (25).

In general

$$-i \int dr'' G(r, r''; 0^-) G(r'', r'; t < 0) \neq G(r, r'; t < 0) \quad (82)$$

and also

$$i \int dr'' G(r, r''; 0^-) G(r'', r'; t > 0) \neq 0. \quad (83)$$

unless $G = G_0$. This implies that if only the exchange part is considered, neglecting the correlation and vertex terms, then in general the sum rule is not fulfilled when a renormalized G is used.

2. Correlation hole

It is also evident that the correlation part of the exchange-correlation hole gives no contribution to the sum rule. The reason for this can be seen by considering the change in the charge density under a perturbation:

$$\delta\rho(1) = \int d2 \chi(1, 2) \delta\varphi(2), \quad (84)$$

where χ is the linear density response function as defined in Eq. (14). A constant perturbation, $\delta\varphi = 1$, does not alter the density so that

$$\int d2 \chi(1, 2) = 0. \quad (85)$$

This property is fulfilled by the RPA response function calculated using G_0 as shown below.

It is interesting to observe that in the case of the electron gas, it can be seen explicitly from Eq. (B5) in Appendix B that the integral of A_1 over r'' is zero since $k \neq k'$ and the same conclusion holds for A_2 , B_1 , and B_2 . Hence the sum-rule is fulfilled, irrespective of the approximation used for $K(q, \omega)$.

Since the response function can be expanded in powers of the polarization P ,

$$\chi = P + PvP + \dots \quad (86)$$

it follows that if the polarization function fulfills

$$\int d2P(1, 2) = 0 \quad (87)$$

then Eq. (85) is satisfied.

The polarization in the RPA is given by

$$P(r, r'; t) = -iG(r, r'; t)G(r', r; -t). \quad (88)$$

If a non-interacting G is used, then Eq. (87) and consequently Eq. (85) are fulfilled. This can be understood as follows. It can be shown that

$$\int dr'' G_0(r, r''; t)G_0(r'', r'; -t) = 0 \quad (89)$$

by using the definition of G_0 :

$$\begin{aligned} & \int dr'' G_0(r, r''; t)G_0(r'', r'; -t) \\ &= \theta(t) \int dr'' \langle \hat{\psi}(rt) \hat{\psi}^\dagger(r'') \rangle \langle \hat{\psi}^\dagger(r') \hat{\psi}(r'', -t) \rangle \\ &+ \theta(-t) \int dr'' \langle \hat{\psi}^\dagger(r'') \hat{\psi}(rt) \rangle \langle \hat{\psi}(r'', -t) \hat{\psi}^\dagger(r') \rangle. \end{aligned} \quad (90)$$

Since the expectation value is taken with respect to a single Slater determinant, the integral over r'' amounts to

$$\int dr'' \varphi_k^*(r'') \varphi_{k'}(r'') = 0, \quad (91)$$

where $\{\varphi_k\}$ is a set of orbitals defining the single Slater determinant, and if k corresponds to an occupied state then k' corresponds to an unoccupied state and vice versa.

However, if a renormalized G is used to calculate P in the RPA as in Eq. (88), the conditions in Eq. (87) and consequently Eq. (85) are no longer fulfilled in general. Thus, with a renormalized G , both the exchange and correlation terms would violate the sum rule, and it seems unlikely that the sum of these two terms would fulfill the sum rule. This might explain why it is not favorable to use a renormalized G in the RPA and consequently in the GW approximation^{2,6}. It also implies that inclusion of the vertex $\delta\Sigma/\delta\varphi$ would restore the sum rule. Hence to preserve the sum rule, the use of a renormalized G should be accompanied by inclusion of the vertex.

3. A simple vertex correction

The preceding consideration suggests a scheme for an approximate vertex correction that would preserve the

sum rule. Consider the following screened-exchange self-energy,

$$\Sigma(1, 2) = iG_0(1, 2)W_0(1, 2), \quad (92)$$

where $W_0(1, 2)$ is an instantaneous interaction,

$$W_0(1, 2) = W_0(r_1, r_2)\delta(t_1 - t_2), \quad (93)$$

with $W_0(r_1, r_2)$ being some screened interaction, e.g., the Thomas-Fermi screened interaction or the static screened interaction calculated within RPA. By using G_0 throughout, the vertex correction is given by

$$\begin{aligned} \frac{\delta\Sigma(1, 2)}{\delta\varphi(3)} &= i \frac{\delta G_0(1, 2)}{\delta\varphi(3)} W_0(1, 2) \\ &= -i \int d4d5 G_0(1, 4) \frac{\delta G_0^{-1}(4, 5)}{\delta\varphi(3)} G_0(5, 2) W_0(1, 2), \end{aligned} \quad (94)$$

where the identity $\delta G = -G(\delta G^{-1})G$ has been utilised and $\frac{\delta W_0}{\delta\varphi} = 0$ since it is assumed that W_0 is fixed. In the presence of the probing field φ , G_0 fulfills the equation of motion

$$\left(i \frac{\partial}{\partial t_1} - h(1) - \varphi(1) \right) G_0(1, 2) = \delta(1 - 2), \quad (95)$$

so that

$$\frac{\delta G_0^{-1}(4, 5)}{\delta\varphi(3)} = -\delta(4 - 5) \left[\delta(3 - 4) + \frac{\delta V_H(4)}{\delta\varphi(3)} \right]. \quad (96)$$

This leads to

$$\begin{aligned} \frac{\delta\Sigma(1, 2)}{\delta\varphi(3)} &= iG_0(1, 3)G_0(3, 2)W_0(1, 2) \\ &+ i \int d4 G_0(1, 4) \frac{\delta V_H(4)}{\delta\varphi(3)} G_0(4, 2)W_0(1, 2), \end{aligned} \quad (97)$$

and hence according to Eqs. (85) and (89),

$$\int d3 \frac{\delta\Sigma(1, 2)}{\delta\varphi(3)} = 0, \quad (98)$$

noting that $t_1 = t_2$ due to the instantaneous interaction. It follows that the vertex in Eq. (97) preserves the sum rule.

G. A model Green function for the interacting electron gas

To assist in analyzing the results of the calculations of V_{xc} of the electron gas, a model Green function has been constructed. A physically motivated model for the Green function of the interacting electron gas is given by the following:

$$\begin{aligned} G(R, t < 0) &= \frac{i}{\Omega} \sum_{k \leq k_F} [Z_k + (1 - Z_k)e^{i\omega_k t}] \\ &\times e^{-iE_k t} e^{i\mathbf{k} \cdot \mathbf{R}}, \end{aligned} \quad (99)$$

$$G(R, t > 0) = -\frac{i}{\Omega} \sum_{k > k_F} [Z_k + (1 - Z_k)e^{-i\omega_k t}] \times e^{-iE_k t} e^{i\mathbf{k} \cdot \mathbf{R}}, \quad (100)$$

where E_k is the quasiparticle energy, Z_k is the quasiparticle renormalization factor, and ω_k is the plasmon energy. To allow for analytic derivation of the exchange-correlation potential, Z_k and ω_k are assumed to be independent of k and E_k is taken to be a renormalized free-electron gas dispersion:

$$Z_k = Z, \quad \omega_k = \omega_p, \quad E_k = \alpha \varepsilon_k = \frac{\alpha}{2} k^2. \quad (101)$$

For an electron gas of density ρ_0 the plasmon energy is given in Eq. (42).

The model Green function can be improved by including the possibility of having spectral weight above or below the Fermi level for $k \leq k_F$ or $k > k_F$, respectively:

$$G(R, t < 0) = \frac{i}{\Omega} \sum_{k \leq k_F} (C_1 + C_2 + C_3) e^{i\mathbf{k} \cdot \mathbf{R}}, \quad (102)$$

$$G(R, t > 0) = -\frac{i}{\Omega} \sum_{k > k_F} (D_1 + D_2 + D_3) e^{i\mathbf{k} \cdot \mathbf{R}}, \quad (103)$$

where

$$C_1 = Z e^{-iE_k t}, \quad (104)$$

$$C_2 = (1 - \beta_k^-)(1 - Z) e^{-i(E_k - \omega_p)t}, \quad (105)$$

$$C_3 = \beta_k^- (1 - Z) e^{-i(E_F + \omega_p)t}, \quad (106)$$

$$D_1 = Z_p e^{-iE_k t}, \quad (107)$$

$$D_2 = (1 - \beta_k^+)(1 - Z_p) e^{-i(E_k + \omega_p)t}, \quad (108)$$

$$D_3 = \beta_k^+ (1 - Z_p) e^{-i(E_F - \omega_p)t}, \quad (109)$$

in which

$$\beta_k^- = \frac{k}{2k_F} \theta(k_F - k), \quad (110)$$

$$\beta_k^+ = \frac{1}{2} \frac{k_{\max} - k}{k_{\max} - k_F} \theta(k_{\max} - k). \quad (111)$$

For $k > k_{\max}$, the dispersion is taken to be that of the free-electron gas for otherwise the integration over k to infinity would not converge. It means physically that high-energy electrons are free since they do not experience exchange and correlations. To conserve electronic charge, the weight above the Fermi level coming from states smaller than k_F is equated to the weight below the Fermi level coming from states larger than k_F , yielding an upper limit, neglecting the k -dependence of β^\pm ,

$$k_{\max} \approx \left(1 + \frac{1 - Z}{1 - Z_p}\right)^{1/3} k_F \quad (112)$$

above which the spectrum does not have weight below the Fermi level.

For $t \neq 0$, the exchange-correlation potential can be obtained from the equation of motion:

$$V_{xc}(R, t) = \frac{1}{G(R, t)} [i\partial_t - h] G(R, t). \quad (113)$$

Since

$$h \exp(i\mathbf{k} \cdot \mathbf{R}) = \frac{k^2}{2} \exp(i\mathbf{k} \cdot \mathbf{R}) \quad (114)$$

one finds for $t < 0$

$$[i\partial_t - h] G(R, t) = i \frac{1}{\Omega} \sum_{k \leq k_F} (A_1 + A_2 + A_3) e^{i\mathbf{k} \cdot \mathbf{R}}, \quad (115)$$

where

$$A_1 = Z(E_k - \varepsilon_k) e^{-iE_k t}, \quad (116)$$

$$A_2 = (1 - \beta_k^-)(1 - Z)(E_k - \varepsilon_k - \omega_p) e^{-i(E_k - \omega_p)t}, \quad (117)$$

$$A_3 = \beta_k^- (1 - Z)(E_F - \varepsilon_k + \omega_p) e^{-i(E_F + \omega_p)t}. \quad (118)$$

For $t > 0$

$$[i\partial_t - h] G(R, t) = -i \frac{1}{\Omega} \sum_{k > k_F} (B_1 + B_2 + B_3) e^{i\mathbf{k} \cdot \mathbf{R}}, \quad (119)$$

where

$$B_1 = Z_p(E_k - \varepsilon_k) e^{-iE_k t}, \quad (120)$$

$$B_2 = (1 - \beta_k^+)(1 - Z_p)(E_k - \varepsilon_k + \omega_p) e^{-i(E_k + \omega_p)t}, \quad (121)$$

$$B_3 = \beta_k^+ (1 - Z_p)(E_F - \varepsilon_k - \omega_p) e^{-i(E_F - \omega_p)t}. \quad (122)$$

III. RESULTS

The results shown in this section are all expressed in atomic units (a.u.) and correspond to $r_s = 4$. Two pairs of representative times, $t = \pm 34.75$ corresponding to $1/\bar{\varepsilon}$, where $\bar{\varepsilon}$ is the center of the occupied band, and $t = \pm 4.62$ corresponding to the inverse of the plasmon energy, $1/\omega_p$, have been chosen for illustrations. Additional times are also considered as appropriate.

A. Angular dependence of the exchange-correlation hole

In Fig. 2 the real part of the exchange holes for the case $R = 10$, $t = -34.75$, and for three different angles $\theta = 0, \pi/4, \pi/2$ as defined in Fig. 1 are shown. These density fluctuations are due to exchange-only interaction

and correspond to the case when a hole created at $R = 0$ at $t = -34.75$ is to be annihilated later at $R = 10$ at $t = 0$. It can be seen that there are more fluctuations for $\theta = 0$ representing the direction along the line connecting the location where the hole is created at $R = 0$ and the location where the hole is annihilated at $R = 10$. The fluctuations are stronger in the direction towards $R = 10$ from the origin than in the opposite direction, which reflect the preponderance of the hole presence and its effects in the former direction. Indeed, the density fluctuations along the direction perpendicular to the line joining $R = 0$ and $R = 10$ ($\theta = \pi/2$) are found to be the least whereas for the direction $\theta = \pi/4$ they are somewhere in between those of $\theta = 0$ and $\pi/2$. In accordance with discussion in the paragraph following Eq. (15), the exchange hole already fulfills the exact condition in Eq. (6), i.e., $\rho_x(0) = -\rho_0$, where ρ_0 the homogeneous electron gas density.

A similar behavior can be observed for the correlation holes shown in Fig. 2. These density fluctuations arise from the classical Coulomb interaction in response to the creation of a hole and its accompanying exchange hole. The fluctuations are particularly strong along the direction towards $R = 10$ from the origin. According to Eq. (16), the correlation hole at the origin should vanish, which is clearly not the case here. There are two possible explanations for this discrepancy, one being the use of the plasmon-pole approximation and another being the neglect of the vertex term. One may speculate that the vertex term is needed even when the exact response function is used, but to answer this issue in the definitive, calculations employing the full RPA response function are required. It is, however, to be noted that discrepancy may not be as severe as it might appear at first sight because what enters into the exchange-correlation potential is the first moment of the spherical average of the exchange-correlation hole so that contributions at small R are significantly cut down. Numerical calculations of the sum rule show that in accordance with theory the exchange hole alone fulfills the sum rule for $t < 0$ and the correlation hole integrates to zero whereas for $t > 0$ both the exchange and the correlation holes integrate to zero.

B. Time dependence of the exchange-correlation hole

To illustrate the time dependence of the exchange-correlation hole, the exchange holes for two representative times $t = -4.62$ and $t = -34.75$ are shown in Fig. 3 for the case $R = 10$ and $\theta = 0$. A similar result is found for the correlation hole. For a short time scale in which the hole is annihilated at a location well separated from the location where it was created, the fluctuations are much stronger than those of a long period. As a guide, it is useful to consider the limit of $R = 0$ and $t = 0^-$, which yields the static exchange-correlation hole.

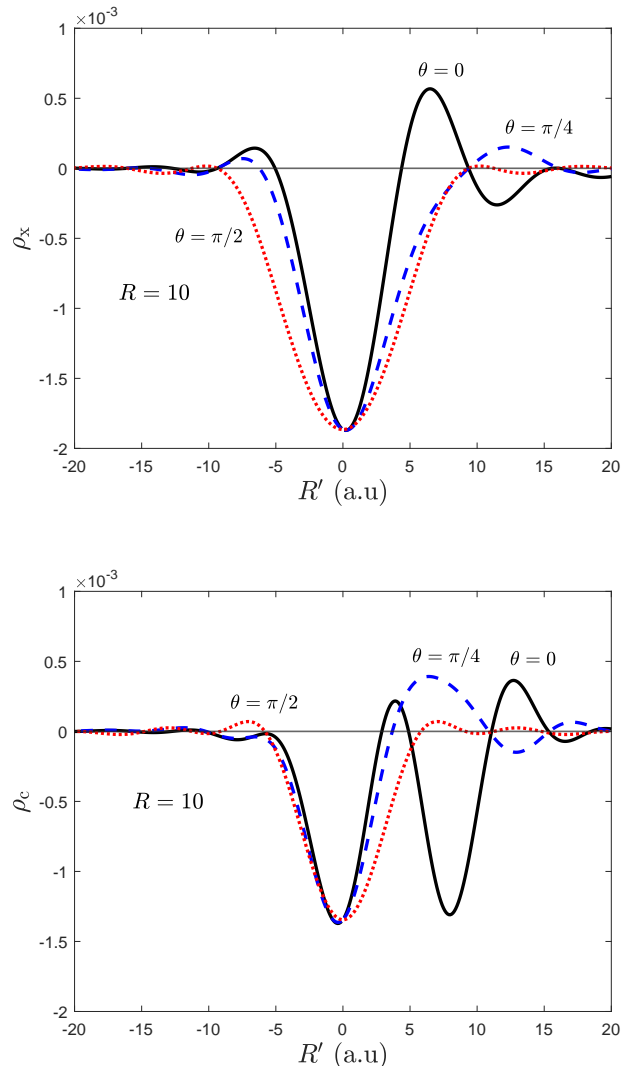


FIG. 2: The real part of the exchange hole (top) and the correlation hole (bottom) for $\theta = 0$ (solid black), $\pi/4$ (dashed blue), and $\pi/2$ (dotted red) for the case $R = 10$ and $t = -34.75$.

There is a correlation between the spatial separation R and the time period, which determines the behavior of the exchange-correlation hole. Within a short period of time but with large R , the system may not have sufficient time to relax so that the density fluctuations arising from a sudden creation of a hole at $t = -4.62$ have not stabilized. These large density fluctuations for small θ , however, contribute little to the exchange-correlation potential since only the spherical average of the exchange-correlation hole is needed and when taking the spherical average each angular contribution is multiplied by $\sin \theta$.

On the other hand, for a relatively short spatial separation $R = 2$, the time-dependence has a much less influence on the exchange hole, as can be seen in Fig. 4.

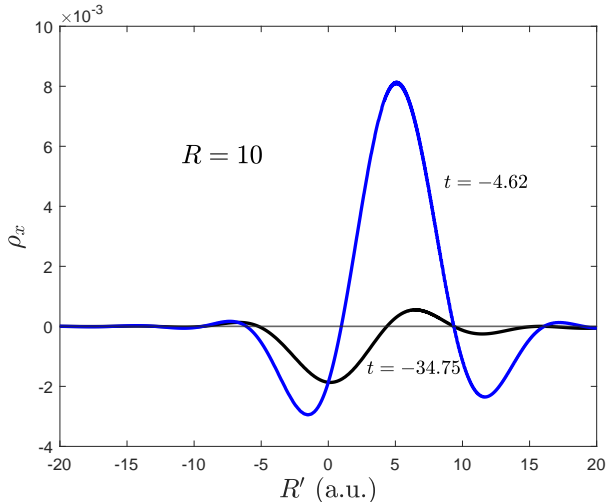


FIG. 3: The real part of the exchange hole for $t = -4.62$ and -34.75 and the case $R = 10$, $\theta = 0$.

The difference between the exchange holes for $t = -4.62$ and -34.75 is much less pronounced than for the case of $R = 10$. The case of small R and small t approaches the static exchange-correlation hole limit of $R = 0$ and $t = 0^-$.

For $t > 0$ corresponding to an electron addition, the exchange hole exhibits a more oscillatory behavior than for $t < 0$. This can be understood from the exact sum rule which dictates that the exchange hole must integrate to zero for $t > 0$. For larger t , however, the oscillations become damped as the system stabilizes itself.

C. Spherical average of the exchange-correlation hole

The relevant quantity determining the exchange-correlation potential is the first radial moment of the spherical average of the exchange-correlation holes. In the upper panel of Fig. 5 the spherical average of the real part of the exchange hole multiplied by R' is shown for several values of R and t . When taking a spherical average the factor $\sin\theta$ implies that the angular region around $\theta \approx 0$ contributes significantly less than the region around $\theta \approx \pi/2$. This is confirmed by comparing Fig. 5 and Fig. 4 for $R = 2$ in which it can be seen that the behavior of the spherical average essentially follows that of the exchange hole for $\theta = \pi/2$.

For $R = 2$ and $t = -4.62$ the exchange hole is virtually indistinguishable from the static Hartree-Fock exchange hole. As expected, the exchange hole for small R and t should approach the static exchange hole. However, even for large values of R and t the exchange hole still follows closely the static one, as can be seen in the top panel of

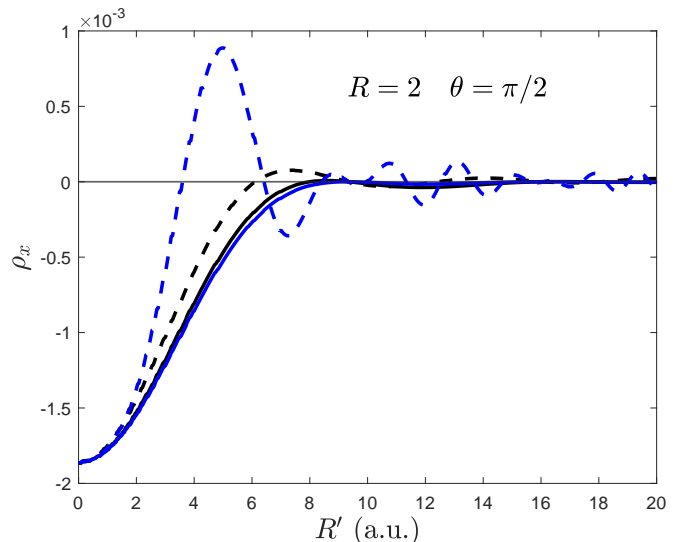


FIG. 4: The real part of the exchange hole for $t = \pm 4.62$ (blue) and ± 34.75 (black) for $R = 2$, $\theta = \pi/2$. The solid and dashed lines correspond to $t < 0$ and $t > 0$, respectively.

Fig. 5. As R is increased, some weight is transferred from the small to the large regions of R' and the exchange hole appears to become less dependent on t for large R .

The spherical average of the correlation hole for several values of R and t is shown in the lower panel of Fig. 5. The general behavior of the correlation hole is similar to that of the exchange hole, except for $R = 2$ in which the correlation hole fluctuates strongly around the origin as a function of time than the corresponding exchange hole. As also expected from the sum rule, which integrates to zero for the correlation hole, more oscillations can be observed than in the corresponding exchange holes. For $t > 0$ the correlation hole tends to be positive around the origin and vanishes as R increases.

The exchange and the correlation holes exhibit strong fluctuations, deviating greatly from the static one at $t = -4.62$, which is found to correlate with the radial distance. To investigate further, the exchange and the correlation holes in the vicinity of $R = 10$ are calculated and shown in Fig. 6. It is quite evident that the large fluctuations at $R = 9 - 10$ correlate with the time $t = -4.62$. These large fluctuations originate from the small values of $|G_0(R, t)|$ at these values of R and t , and are carried over to the exchange-correlation potentials as discussed in the next section.

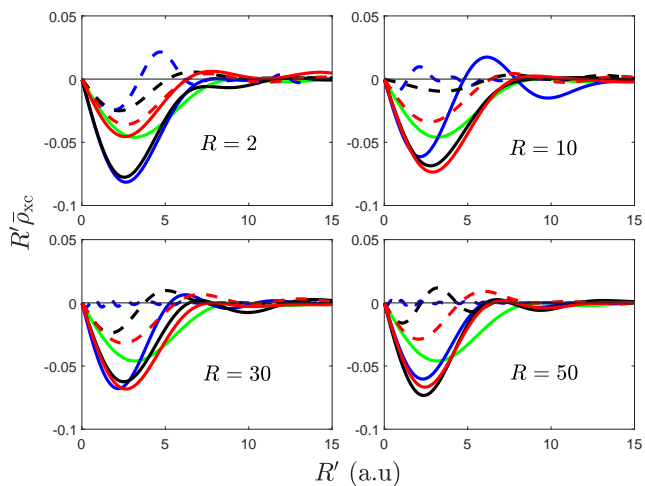
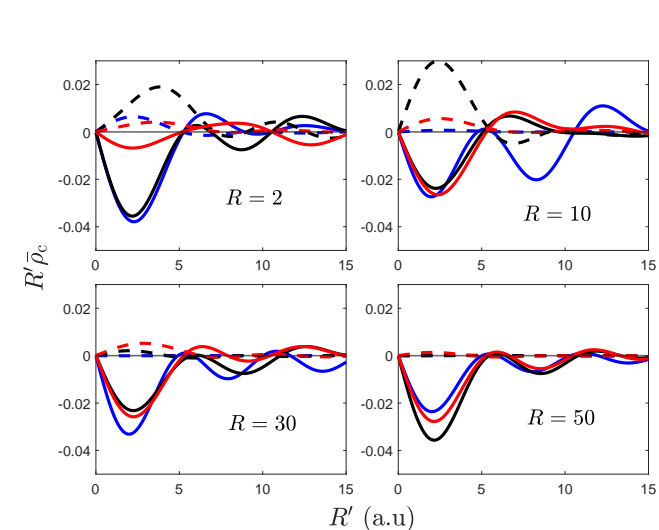
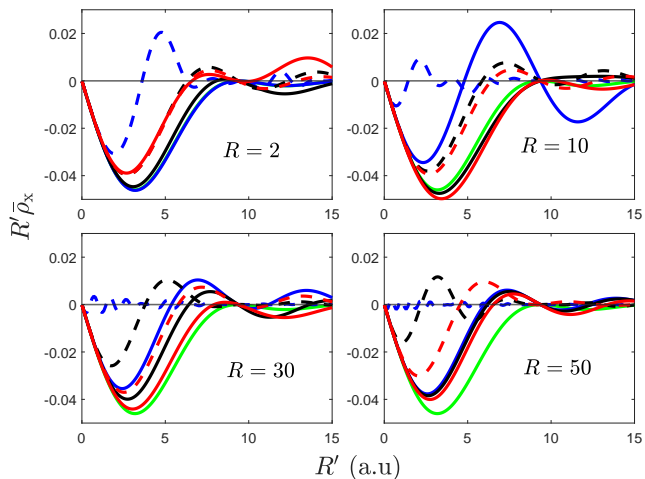


FIG. 5: The real part of the spherical average of the exchange hole (upper panel), the correlation hole (middle panel), and the exchange-correlation hole (lower panel) multiplied by R' for $t = \pm 4.62$ (blue), ± 34.75 (black), ± 69.5 (red), and $R = 2, 10, 30, 50$. The solid and dashed curves correspond to $t < 0$ and $t > 0$, respectively. The green curve is the static exchange hole from the Hartree-Fock approximation. For $t = -4.62$ (solid blue) and $R = 2$ the exchange hole is virtually indistinguishable from the static one.

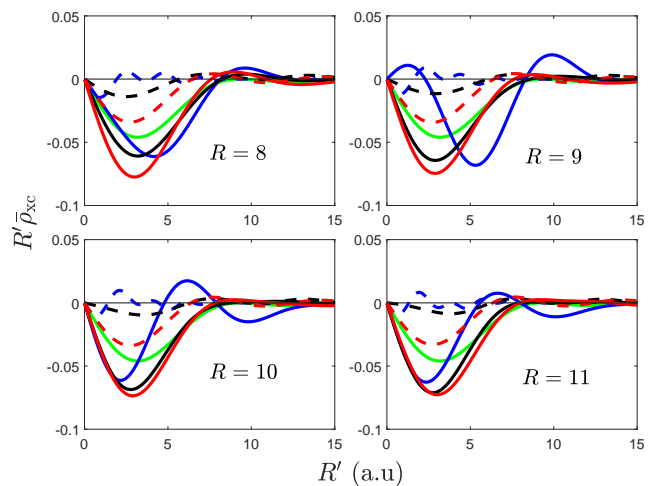
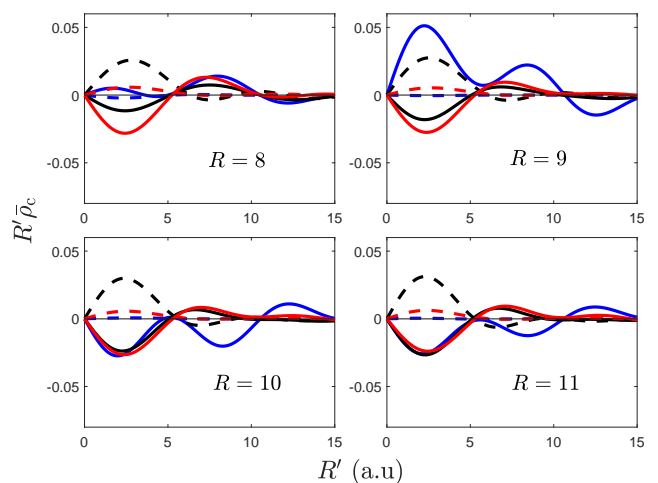
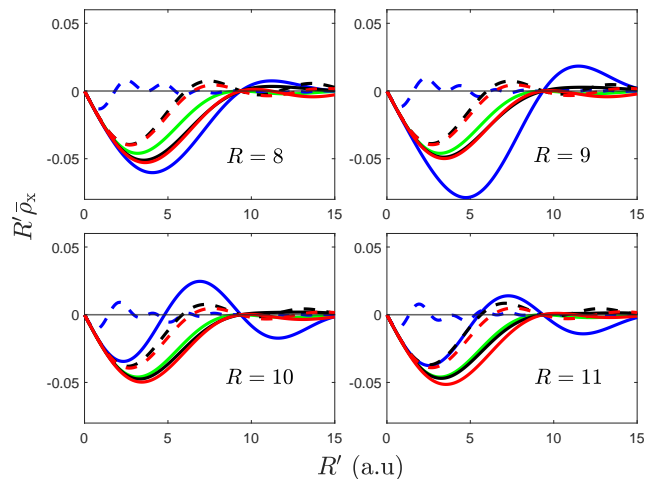


FIG. 6: The real part of the spherical average of the exchange hole (upper panel), the correlation hole (middle panel), and the exchange-correlation hole (lower panel) multiplied by R' for $t = \pm 4.62$ (blue), ± 34.75 (black), ± 69.5 (red), and $R = 8, 9, 10, 11$. The solid and dashed curves correspond to $t < 0$ and $t > 0$, respectively. The green curve is the static exchange hole from the Hartree-Fock approximation.

D. Exchange-correlation potentials

From the spherical average of the exchange-correlation hole the exchange-correlation potential can be determined. The real and imaginary parts of the exchange potential for $t = \pm 4.62$ and ± 34.75 are shown in Figs. 7 and 8, respectively. For $t < 0$ there is a striking difference between the exchange potentials corresponding to the two times. The exchange potential corresponding to $t = -4.62$ exhibits a pronounced structure around $R = 9$ and 16, whereas the one corresponding to $t = -34.75$ is almost constant with a relatively weak feature. As mentioned earlier, this strong structure at $t = -4.62$ arises from the small value of $|G_0(R, t)|$ at $R = 9$ and 16 as shown in Fig. 9. In fact, the exchange potential has a strong structure at those positions for a range of t , as can be seen in Fig. 10. The structure is very sharp for very small t and as the magnitude of t increases, it becomes weaker. A plausible explanation is that when a hole is introduced into the system, large density fluctuations arise and within a short period of time the system does not have enough time to relax, generating as a consequence a strong spatial variation in the exchange potential. However, strong spatial variations also appear at a large-time scale as shown in Fig. 11. The common denominator for the presence of strong structures in the exchange-correlation potential is the diminishing value of $|G_0(R, t)|$ at the corresponding position R and time t , as can be seen in Fig. 12.

For $t > 0$ the exchange potentials are generally weaker and less attractive than for $t < 0$ as can be seen in Fig. 7. The difference between the two cases may be traced back to the fundamental physical difference between removing an electron (hole creation, $t < 0$) and adding an electron ($t > 0$), in that the removed electron is part of the system in the ground state whereas the added electron is not. This is also reflected in the sum rule which integrates to -1 for a hole addition but zero for an electron addition. Thus, the exchange potential associated with a hole creation must be stronger than that associated with an electron addition. Aside from special systems that possess a particle-hole symmetry, the creation of a hole can be expected to create a stronger disturbance to the system in the ground state than the addition of an electron.

The exchange potential does not take into account the classical Coulomb response of the electrons which results in screening of the density fluctuations arising from the exchange interaction. In Fig. 7 (middle) the real parts of the correlation potentials associated with the linear density response of the system are shown for the two pairs of representative times $t = \pm 4.62$ and ± 34.75 . As in the case of exchange, the correlation potential corresponding to $t = -4.62$ has a pronounced structure in comparison with the one corresponding to $t = -34.75$.

The real and imaginary parts of the exchange-correlation potentials are displayed in Figs. 7 and 8, respectively. Peaks in the imaginary part of the exchange-

correlation potential, which is the analog of the imaginary part of the self-energy, signals the presence of damping. It is evident that there is a strong cancellation of exchange and correlation. The Kramers-Kronig-like structures in the exchange potential between $R = 8$ and 10 as well as between 15 and 17 in Fig. 7 induce polarization in which electrons and holes are accumulated in opposite regions where the minimum and maximum of V_x are located. This exchange polarization is neutralized by Coulomb screening, which is affected by the presence of inverted structures in V_c at the corresponding regions. This results in a strong cancellation between exchange and correlation potentials and the resulting total exchange-correlation potential has a much less structure than both the exchange and the correlation potentials.

To illustrate further the large cancellation between exchange and correlation, the real part of the exchange, correlation, and exchange-correlation potentials for $t = -1$ are displayed in Fig. 13. It is tempting to speculate that the remaining structure in the exchange-correlation potential might be smoothed out when full RPA calculations are carried out without relying on the plasmon-pole approximation. A similar cancellation is also found for $t = -34.75$ (Fig. 7) but to a much lesser extent since both the exchange and the correlation potentials have little structures to begin with.

The strong cancellation between exchange and correlation is well known in the self-energy formalism. The cancellation manifests itself in the one-particle dispersion in which the too large occupied bandwidth within the Hartree-Fock approximation is significantly reduced by correlation effects, resulting in a dispersion close to the non-interacting one. The V_{xc} formalism, however, offers a different perspective in which the cancellation can be explicitly seen in the exchange-correlation potential in space and time.

R	9	5	9	16	5
t	0 to -5	-60	-84	-102	-114

TABLE I: The approximate values of $R \leq 20$ and the corresponding times $t \leq 0$ around which strong structures are found in the exchange and the correlation potentials and strong deviations in the exchange and the correlation holes from their static counterparts are observed.

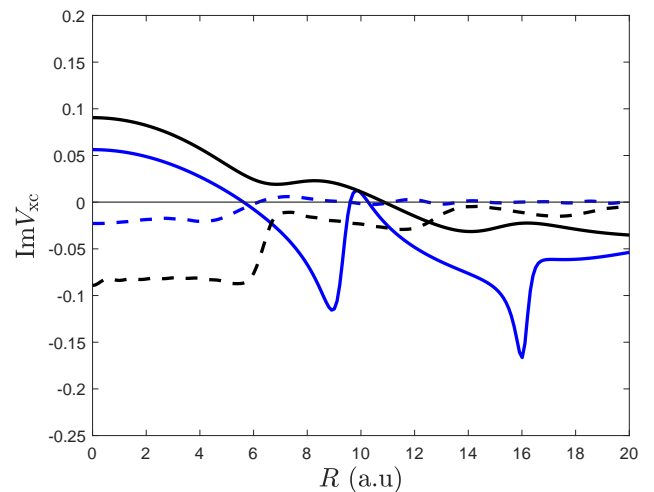
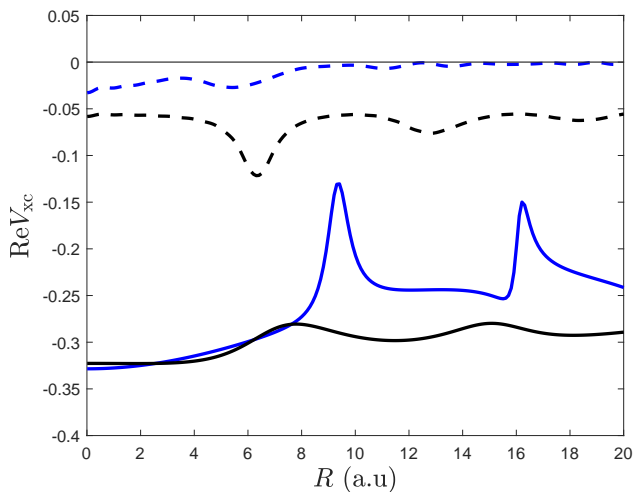
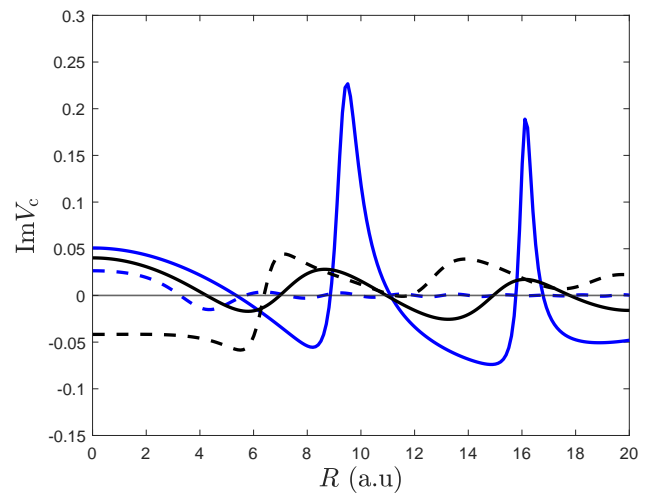
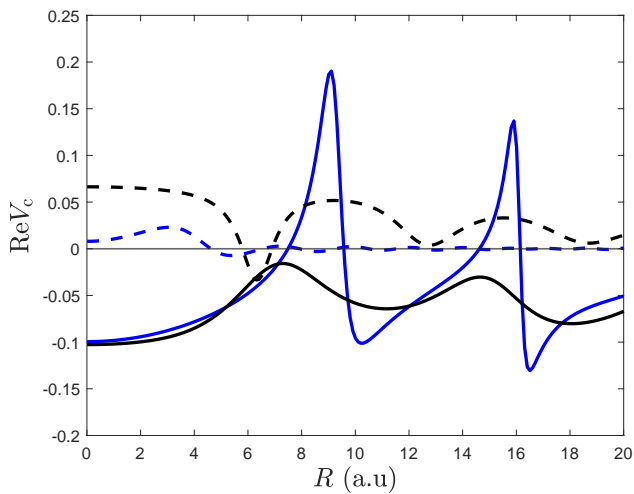
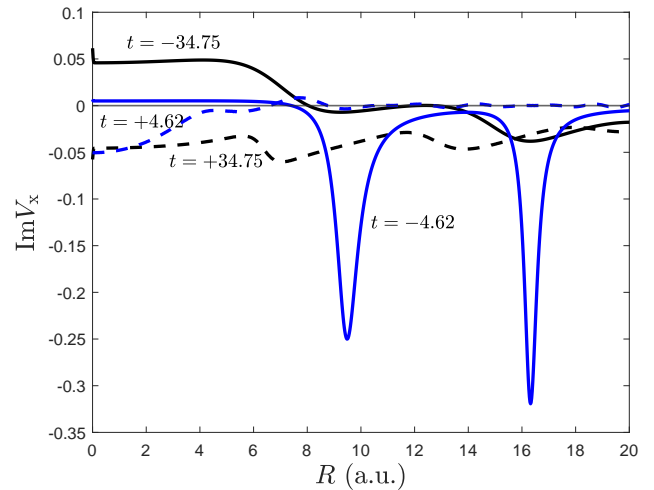
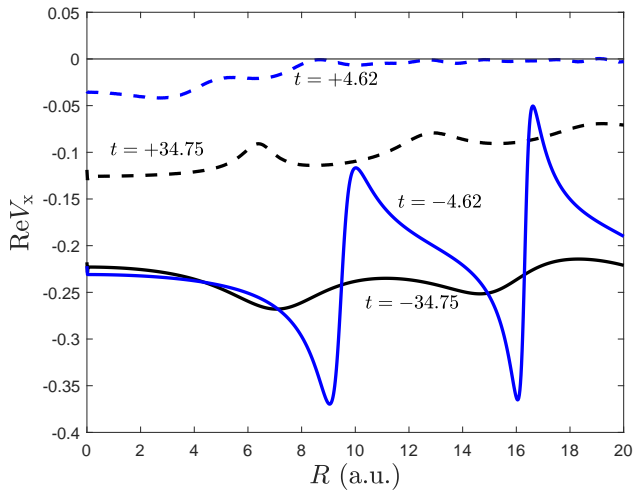


FIG. 7: The real part of the exchange potential (top), the correlation potential (middle), and the exchange-correlation potential for $t = \pm 4.62$ (blue) and ± 34.75 (black). The solid and dashed curves correspond to $t < 0$ and $t > 0$, respectively.

FIG. 8: The imaginary part of the exchange potential (top), the correlation potential (middle), and the exchange-correlation potential (bottom) for $t = \pm 4.62$ (blue) and ± 34.75 (black). The solid and dashed curves correspond to $t < 0$ and $t > 0$, respectively.

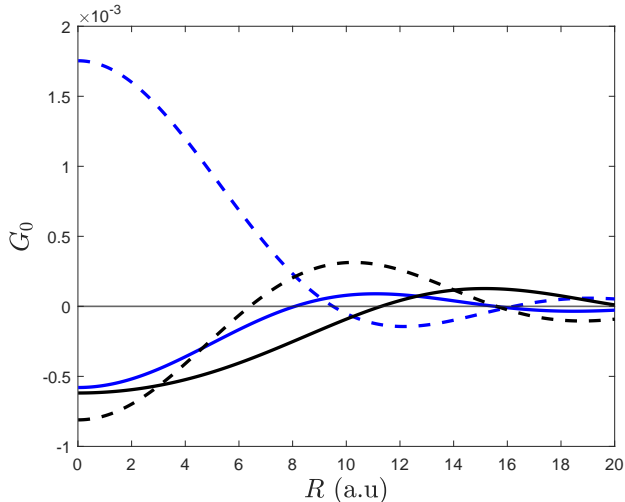


FIG. 9: The real (solid) and the imaginary (dashed) parts of the non-interacting Green function for $t = -4.62$ (blue) and -34.75 (black). For $t = -4.62$, the value of $|G_0|$ is close to zero at positions $R = 9$ and 16 , whereas for $t = -34.75$, it remains relatively substantial.

E. Comparison with the model Green function

To check the electron gas results and to gain more insight into the salient features of the exchange-correlation potentials, a model Green function has been constructed as described in Sec. II G. The exchange-correlation potentials derived from the model for $t = \pm 4.62$ and $t = \pm 34.75$ are shown in Fig. 14, which should be compared with Fig. 7. Apart from the absolute position, which cannot be determined without calculating the quasiparticle dispersion from the resulting electron gas exchange-correlation potential, the agreement for $t = \pm 34.75$ is quite striking. There is a discrepancy in the separation between $V_{xc}(t > 0)$ and $V_{xc}(t < 0)$, which may indicate an overestimation of correlation within the plasmon-pole approximation. Increasing the range of integration from $2k_F$ to $4k_F$ in the integration over the unoccupied states results in a down shift of the correlation potential while the shape remains stable. There is less agreement for $t = \pm 4.62$, both concerning the shape as well as the separation between $V_{xc}(t > 0)$ and $V_{xc}(t < 0)$. Again, this may be due to the plasmon-pole approximation, or, speculatively speaking, to the model itself, which may not be accurate for small t . The small time behavior is determined by the quality of the model at high energy. The model assumes a sharp plasmon excitation, which may be valid for small momentum but becomes less accurate at large momenta beyond the critical momentum.

To make a separate comparison of both V_x and V_C , the exchange potential deduced from the Hartree-Fock Green function is calculated and used to determine the correla-

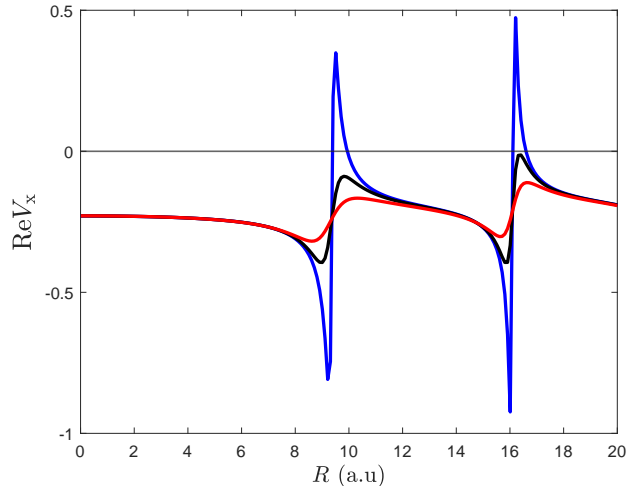


FIG. 10: The real part of the exchange potential for $t = -1$ (blue), -4 (black) and -8 (red). The structure at $R = 9$ and 16 becomes sharper as $t \rightarrow 0^-$, which, however, is largely cancelled by the correlation potential, as illustrated in Fig. 13.

tion potential of the model by subtracting the exchange potential from the total exchange-correlation potential. The results are shown in Fig. 15 for $t = \pm 4.62$ and $t = \pm 34.75$. Here, there is no ambiguity regarding the absolute position of the exchange potentials. The close agreement between the exchange potential deduced from the Hartree-Fock Green function and the one calculated from Eqs. (61) and (62) for the electron gas attests that the physical interpretation of the exchange-correlation hole in Eq. (15), in which the first term on the right-hand side is associated with the exchange hole, is well motivated.

IV. CONCLUSION AND SUMMARY

The exchange-correlation hole and potential of the homogeneous electron gas have been studied within the RPA for $r_s = 4$ and several representative time periods. The angular dependence of the exchange-correlation hole for $t < 0$ shows a stronger oscillation along the line joining the location where the hole is created and the location where the hole is annihilated ($\theta = 0$) whereas along the perpendicular direction ($\theta = \pi/2$) it shows the least oscillation. This behavior can be attributed to the degree of preponderance of the hole along the respective directions.

The behavior of the exchange and the correlation holes reveals a correlation between the separation R and the time period t . For certain values of R large fluctuations are found within a range of time. This behaviour is mimicked by the exchange and the correlation potentials

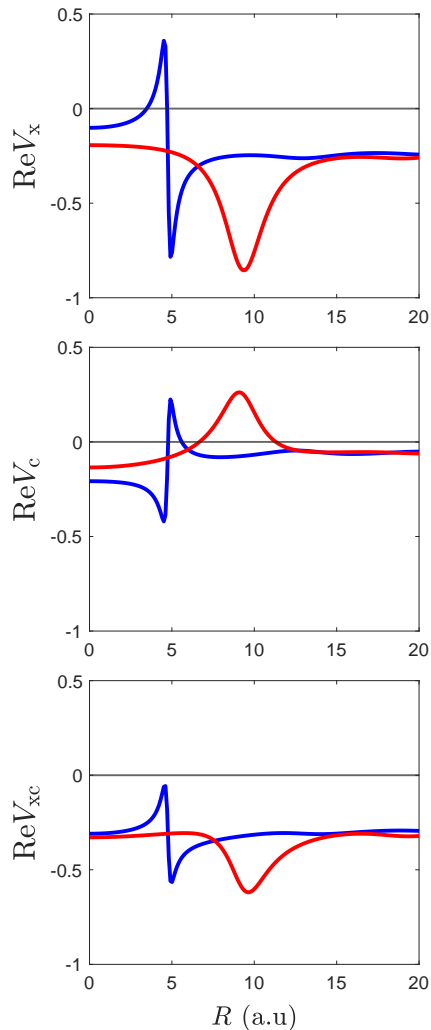


FIG. 11: The real part of the exchange potential (top), the correlation potential (middle), and the exchange-correlation potential (bottom) for $t = -60$ (blue) and -84 (red).

and is found to originate from the diminishing value of $|G_0(R, t)|$ at the respective position and time.

The spherical average of the exchange-correlation hole for $t < 0$ is generally larger than for $t > 0$, which is a consequence of the sum rule being -1 for the former and 0 for the latter. This property is inherited by the exchange-correlation potential, since it is determined by the first radial moment of the spherical average of the exchange-correlation hole. It is found that the exchange potential in space and time is substantially cancelled by the correlation potential, which maybe seen as the analog of the well-known cancellation of the Fock exchange and the correlation self-energy of the electron gas in momentum and frequency. The strong cancellation results in an exchange-correlation potential with much less structure than in the corresponding exchange and correlation po-

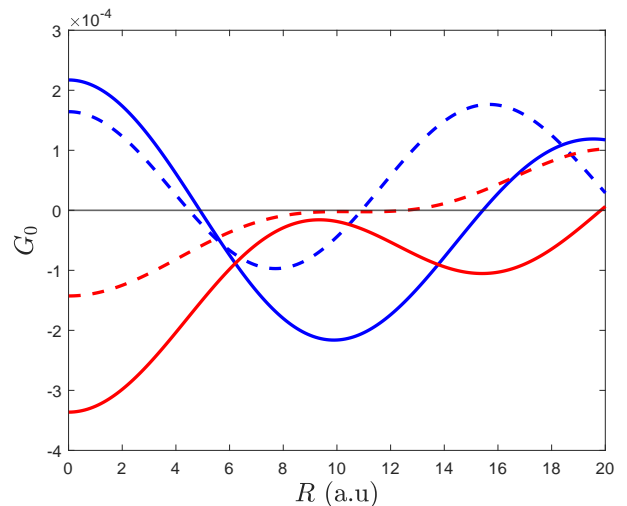


FIG. 12: The real (solid) and the imaginary (dashed) parts of the non-interacting Green function for $t = -60$ (blue) and -84 (red).

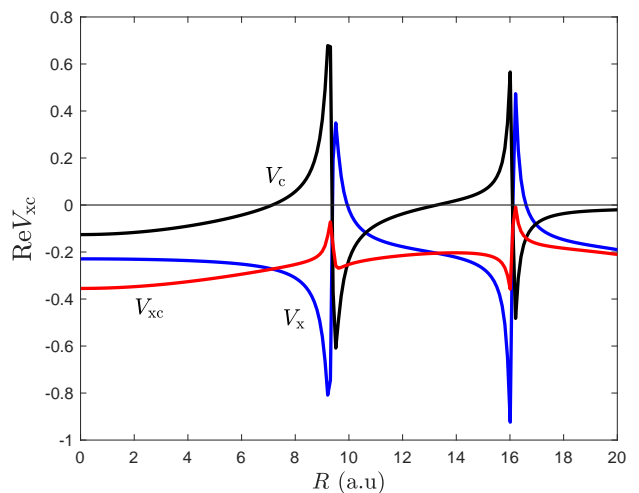


FIG. 13: The real part of the exchange potential (blue), the correlation potential (black), and the exchange-correlation potential (red) for $t = -1$. The large cancellation between exchange and correlation can be clearly seen.

tentials. This encouraging result lends support for the feasibility of applying the local density approximation.

Analysis of the sum rule offers a physical explanation why using a non-interacting Green function is more advantageous than using a renormalized one when calculating the response function in RPA and consequently in calculating the self-energy within the GW approximation. A simple vertex correction that preserves the sum

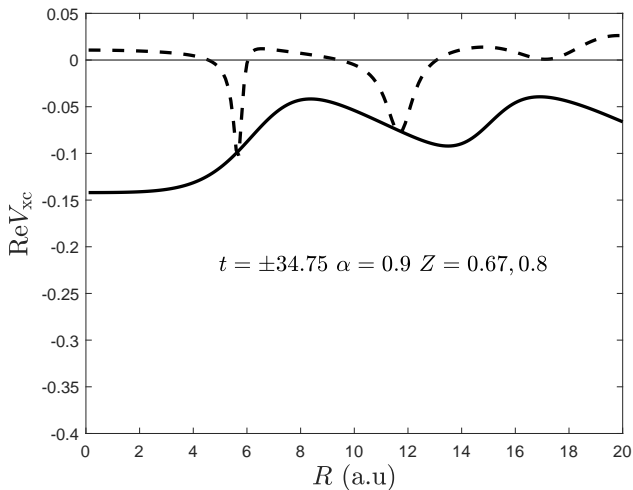
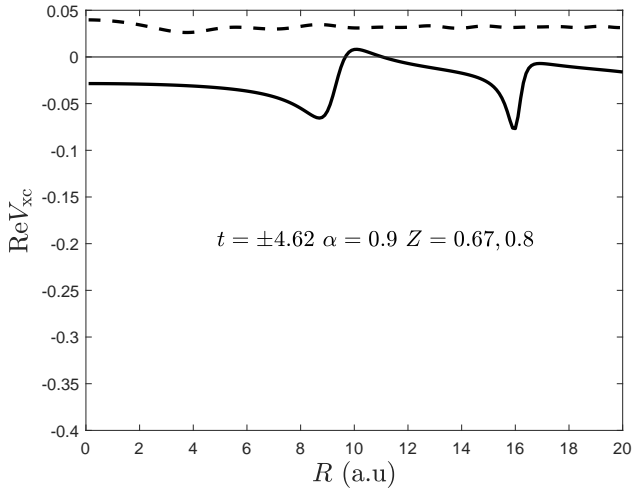


FIG. 14: The real part of the exchange-correlation potential for $t = \pm 4.62$ (top) and $t = \pm 34.75$ (bottom) from the model Green function. The solid and dashed curves correspond to $t < 0$ and $t > 0$, respectively. The parameters used are indicated in the figure. Two different values of renormalization factors Z are used, one for $t < 0$ ($Z = 0.67$) and one for $t > 0$ ($Z_p = 0.8$). The choice of the parameters is based on the GW results.

rule is then proposed.

The present work provides a starting point for more accurate calculations of the exchange-correlation hole and potential of the electron gas. The plasmon-pole approximation is not expected to yield accurate results since it neglects the limits in the solid angles. Nevertheless, comparison with results obtained from a model Green function suggests that it captures the main features of the exchange-correlation potential. It would be highly desirable to perform full RPA calculations without em-

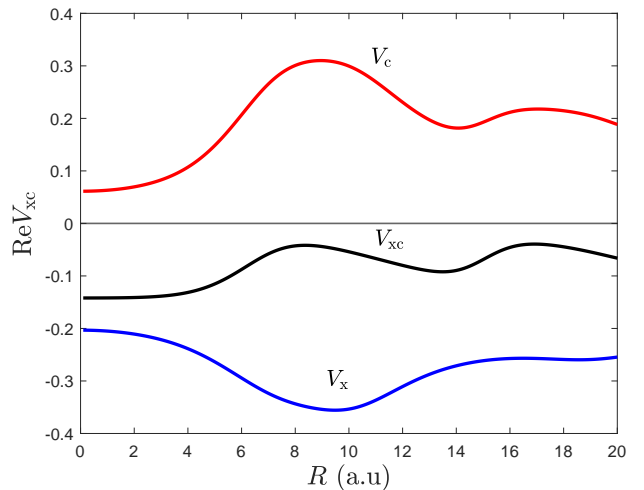
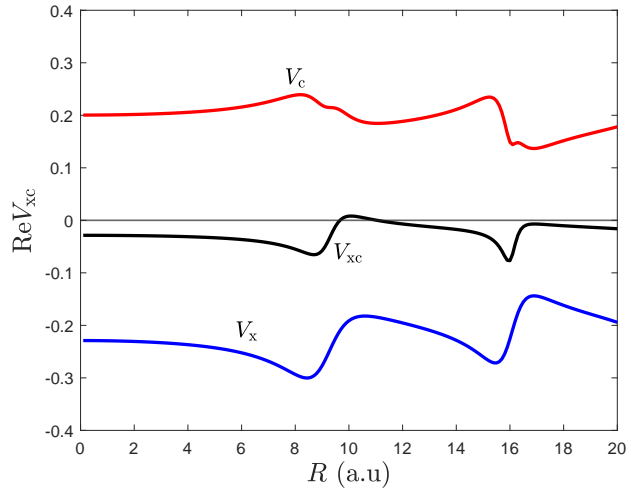


FIG. 15: The real part of the exchange potential V_x (blue) derived from the Hartree-Fock Green function and the exchange-correlation potential V_{xc} (black) from the model Green function for $t = -4.62$ (top) and $t = -34.75$ (bottom). The correlation potential (red) is defined as $V_c = V_{xc} - V_x$.

ploying the plasmon-pole approximation with the aim of constructing a local-density type approximation for the exchange-correlation potential, which can be applied to calculate the Green function of real materials, circumventing computationally expensive traditional self-energy calculations based on Feynman diagrams and path integral techniques.

Acknowledgments

Financial support from the Knut and Alice Wallenberg (KAW) Foundation (Grant number 2017.0061) and

the Swedish Research Council (Vetenskapsrådet, VR, Grant number 2021_04498) is gratefully acknowledged. We thank Rex Godby for valuable discussions.

Appendix A: Calculation of $G_0(R, t > 0)$

The integral over k in $G_0(R, t > 0)$ can be decomposed as follows:

$$\int_{k_F}^{\infty} dk = \int_0^{\infty} dk - \int_0^{k_F} dk. \quad (\text{A1})$$

$$iG_0(R, t > 0) = \frac{1}{2\pi^2 R} \{I(0, \infty) - I(0, k_F)\}, \quad (\text{A2})$$

where

$$I(a, b) = \int_a^b dk k \sin(kR) e^{-ik^2 t/2}. \quad (\text{A3})$$

Consider the following integral

$$\int_{-\infty}^{\infty} dk k e^{ikR} e^{-ik^2 t/2} = e^{iR^2/2t} \int_{-\infty}^{\infty} dk k e^{-i(k-R/t)^2 t/2}. \quad (\text{A4})$$

By making a change of variable,

$$k - \frac{R}{t} = \sqrt{\frac{2}{t}} x, \quad (\text{A5})$$

the integral $I(0, \infty)$ can be performed analytically yielding

$$I(0, \infty) = \sqrt{\frac{\pi}{2it}} \frac{R}{it} e^{iR^2/2t}. \quad (\text{A6})$$

For $t \rightarrow 0^+$, by introducing a converging factor $e^{-|\alpha|q}$ one finds,

$$\lim_{\alpha \rightarrow 0} \int_0^{\infty} dk k \sin(kR) e^{-|\alpha|q} = 0 \quad (\text{A7})$$

implying that indeed $G_0(R, 0^+) = G_0(R, 0^-)$ for $R \neq 0$.

Appendix B: Correlation hole

From Eq. (15), the correlation hole is given by the following equation:

$$\begin{aligned} \rho_c(r, r', r''; t) G(r, r'; t) = \\ i \int dr_4 dt_4 G(r, r_4; t - t_4) K(r_4, r''; t_4 - t) G(r_4, r'; t_4). \end{aligned} \quad (\text{B1})$$

A non-interacting G is used,

$$\begin{aligned} G_0(r - r_4, t - t_4) = \frac{i}{\Omega} \sum_{k \leq k_F} e^{i\mathbf{k} \cdot (\mathbf{r} - \mathbf{r}_4)} e^{-i\varepsilon_k(t - t_4)} \theta(t_4 - t) \\ - \frac{i}{\Omega} \sum_{k > k_F} e^{i\mathbf{k} \cdot (\mathbf{r} - \mathbf{r}_4)} e^{-i\varepsilon_k(t - t_4)} \theta(t - t_4), \end{aligned} \quad (\text{B2})$$

$$\begin{aligned} G_0(r_4 - r', t_4) = \frac{i}{\Omega} \sum_{k' \leq k_F} e^{i\mathbf{k}' \cdot (\mathbf{r}_4 - \mathbf{r}')} e^{-i\varepsilon_{k'} t_4} \theta(-t_4) \\ - \frac{i}{\Omega} \sum_{k' > k_F} e^{i\mathbf{k}' \cdot (\mathbf{r}_4 - \mathbf{r}')} e^{-i\varepsilon_{k'} t_4} \theta(t_4), \end{aligned} \quad (\text{B3})$$

and

$$\begin{aligned} K(r_4 - r'', t_4 - t) \\ = \frac{1}{\Omega} \sum_q \int \frac{d\omega}{2\pi} e^{-i\mathbf{q} \cdot (\mathbf{r}_4 - \mathbf{r}'')} e^{-i\omega(t_4 - t)} K(q, \omega). \end{aligned} \quad (\text{B4})$$

Consider the right-hand side of Eq. (B1) and the case $t < 0$. From the product of the two Green functions one obtains four terms but only two survive. The first non-zero term is (note the additional factor of i from $iGKG$)

$$\begin{aligned} A_1 = -\frac{i^3}{\Omega^3} \sum_{k \leq k_F} \sum_{k' > k_F} e^{i\mathbf{k} \cdot \mathbf{r}} e^{-i\mathbf{k}' \cdot \mathbf{r}'} \\ \times \sum_q e^{i\mathbf{q} \cdot \mathbf{r}''} \int \frac{d\omega}{2\pi} e^{i(\omega - \varepsilon_k)t} K(q, \omega) \\ \times \int dr_4 e^{-i(\mathbf{k} - \mathbf{k}' + \mathbf{q}) \cdot \mathbf{r}_4} \int_0^{\infty} dt_4 e^{-i(\omega - \varepsilon_k + \varepsilon_{k'} - i\eta)t_4} \\ = \frac{1}{\Omega^2} \sum_{k \leq k_F} \sum_{k' > k_F} e^{i\mathbf{k} \cdot \mathbf{r}} e^{-i\mathbf{k}' \cdot \mathbf{r}'} e^{i(\mathbf{k}' - \mathbf{k}) \cdot \mathbf{r}''} \\ \times \int \frac{d\omega}{2\pi} K(|\mathbf{k}' - \mathbf{k}|, \omega) \frac{e^{i(\omega - \varepsilon_k)t}}{\omega - \varepsilon_k + \varepsilon_{k'} - i\eta}, \end{aligned} \quad (\text{B5})$$

which can be rewritten in terms of the radial variables:

$$\begin{aligned} A_1 = \frac{1}{\Omega^2} \sum_{k \leq k_F} e^{-i\mathbf{k} \cdot \mathbf{R}'} \sum_{k' > k_F} e^{i\mathbf{k}' \cdot \mathbf{R}''} \\ \times \int \frac{d\omega}{2\pi} K(|\mathbf{k}' - \mathbf{k}|, \omega) \frac{e^{i(\omega - \varepsilon_k)t}}{\omega - \varepsilon_k + \varepsilon_{k'} - i\eta}. \end{aligned} \quad (\text{B6})$$

The second non-zero term is similar to the first and given by

$$\begin{aligned} A_2 = -\frac{1}{\Omega^2} \sum_{k > k_F} e^{-i\mathbf{k} \cdot \mathbf{R}'} \sum_{k' \leq k_F} e^{i\mathbf{k}' \cdot \mathbf{R}''} \\ \times \int \frac{d\omega}{2\pi} K(|\mathbf{k}' - \mathbf{k}|, \omega) \frac{e^{-i\varepsilon_{k'} t}}{\omega - \varepsilon_k + \varepsilon_{k'} + i\eta}. \end{aligned} \quad (\text{B7})$$

For the case $t > 0$ similar consideration yields

$$\begin{aligned} B_1 = \frac{1}{\Omega^2} \sum_{k \leq k_F} e^{-i\mathbf{k} \cdot \mathbf{R}'} \sum_{k' > k_F} e^{i\mathbf{k}' \cdot \mathbf{R}''} \\ \times \int \frac{d\omega}{2\pi} K(|\mathbf{k}' - \mathbf{k}|, \omega) \frac{e^{-i\varepsilon_{k'} t}}{\omega - \varepsilon_k + \varepsilon_{k'} - i\eta} \end{aligned} \quad (\text{B8})$$

$$B_2 = -\frac{1}{\Omega^2} \sum_{k>k_F} e^{-i\mathbf{k}\cdot\mathbf{R}'} \sum_{k'\leq k_F} e^{i\mathbf{k}'\cdot\mathbf{R}''} \\ \times \int \frac{d\omega}{2\pi} K(|\mathbf{k}' - \mathbf{k}|, \omega) \frac{e^{i(\omega - \varepsilon_k)t}}{\omega - \varepsilon_k + \varepsilon_{k'} + i\eta}. \quad (\text{B9})$$

To calculate the integral over ω one utilizes the spectral representation of K :

$$K(k, \omega) = \int_{-\infty}^0 d\omega' \frac{L(k, \omega')}{\omega - \omega' - i\delta} + \int_0^{\infty} d\omega' \frac{L(k, \omega')}{\omega - \omega' + i\delta}, \quad (\text{B10})$$

where

$$L(k, \omega) = -\frac{1}{\pi} \text{sign}(\omega) \text{Im}K(k, \omega). \quad (\text{B11})$$

The spectral function $L(k, \omega)$ is an odd function in ω .

For the case $t < 0$ the contour integral for A_1 in the complex ω plane is closed in the lower-half plane yielding

$$\int \frac{d\omega}{2\pi} \frac{1}{\omega - \omega' + i\delta} \times \frac{e^{i(\omega - \varepsilon_k)t}}{\omega - \varepsilon_k + \varepsilon_{k'} - i\eta} \\ = \frac{-ie^{i(\omega' - \varepsilon_k - i\delta)t}}{\omega' - \varepsilon_k + \varepsilon_{k'} - i\eta}. \quad (\text{B12})$$

One obtains, using $L(k, -\omega) = -L(k, \omega)$,

$$A_1 = \frac{1}{\Omega^2} \sum_{k\leq k_F} e^{-i\mathbf{k}\cdot\mathbf{R}'} \sum_{k'>k_F} e^{i\mathbf{k}'\cdot\mathbf{R}''} e^{-i\varepsilon_k t} \\ \times \int_0^{\infty} d\omega' L(|\mathbf{k}' - \mathbf{k}|, \omega') \frac{-ie^{i\omega' t}}{\omega' + \varepsilon_{k'} - \varepsilon_k} \quad (\text{B13})$$

and

$$A_2 = \frac{1}{\Omega^2} \sum_{k>k_F} e^{-i\mathbf{k}\cdot\mathbf{R}'} \sum_{k'\leq k_F} e^{i\mathbf{k}'\cdot\mathbf{R}''} e^{-i\varepsilon_{k'} t} \\ \times \int_0^{\infty} d\omega' L(|\mathbf{k}' - \mathbf{k}|, \omega') \frac{-i}{\omega' + \varepsilon_k - \varepsilon_{k'}}. \quad (\text{B14})$$

For the case $t > 0$ one obtains

$$B_1 = \frac{1}{\Omega^2} \sum_{k\leq k_F} e^{-i\mathbf{k}\cdot\mathbf{R}'} \sum_{k'>k_F} e^{i\mathbf{k}'\cdot\mathbf{R}''} e^{-i\varepsilon_{k'} t} \\ \times \int_0^{\infty} d\omega' L(|\mathbf{k}' - \mathbf{k}|, \omega') \frac{-i}{\omega' + \varepsilon_{k'} - \varepsilon_k} \quad (\text{B15})$$

$$B_2 = \frac{1}{\Omega^2} \sum_{k>k_F} e^{-i\mathbf{k}\cdot\mathbf{R}'} \sum_{k'\leq k_F} e^{i\mathbf{k}'\cdot\mathbf{R}''} e^{-i\varepsilon_k t} \\ \times \int_0^{\infty} d\omega' L(|\mathbf{k}' - \mathbf{k}|, \omega') \frac{-ie^{-i\omega' t}}{\omega' + \varepsilon_k - \varepsilon_{k'}}. \quad (\text{B16})$$

For each t the integral over ω' can be parametrized as follows:

$$M(q, \omega, t) = \int_0^{\infty} d\omega' L(q, \omega') \frac{-ie^{i\omega' t}}{\omega' + \omega}, \quad (\text{B17})$$

so that

$$A_1 = \frac{1}{\Omega^2} \sum_{k\leq k_F} e^{-i\mathbf{k}\cdot\mathbf{R}'} e^{-i\varepsilon_k t} \sum_{k'>k_F} e^{i\mathbf{k}'\cdot\mathbf{R}''} \\ \times M(|\mathbf{k}' - \mathbf{k}|, \varepsilon_{k'} - \varepsilon_k, t); \quad (\text{B18})$$

$$A_2 = \frac{1}{\Omega^2} \sum_{k>k_F} e^{-i\mathbf{k}\cdot\mathbf{R}'} \sum_{k'\leq k_F} e^{i\mathbf{k}'\cdot\mathbf{R}''} e^{-i\varepsilon_{k'} t} \\ \times M(|\mathbf{k}' - \mathbf{k}|, \varepsilon_k - \varepsilon_{k'}, 0); \quad (\text{B19})$$

$$B_1 = \frac{1}{\Omega^2} \sum_{k\leq k_F} e^{-i\mathbf{k}\cdot\mathbf{R}'} \sum_{k'>k_F} e^{i\mathbf{k}'\cdot\mathbf{R}''} e^{-i\varepsilon_{k'} t} \\ \times M(|\mathbf{k}' - \mathbf{k}|, \varepsilon_{k'} - \varepsilon_k, 0); \quad (\text{B20})$$

$$B_2 = \frac{1}{\Omega^2} \sum_{k>k_F} e^{-i\mathbf{k}\cdot\mathbf{R}'} \sum_{k'\leq k_F} e^{i\mathbf{k}'\cdot\mathbf{R}''} e^{-i\varepsilon_k t} \\ \times M(|\mathbf{k}' - \mathbf{k}|, \varepsilon_k - \varepsilon_{k'}, -t). \quad (\text{B21})$$

By defining

$$\gamma(R, R', t, t', t'') = \frac{1}{\Omega^2} \sum_{k\leq k_F} e^{-i\mathbf{k}\cdot\mathbf{R}} e^{-i\varepsilon_k t} \\ \times \sum_{k'>k_F} e^{i\mathbf{k}'\cdot\mathbf{R}'} e^{-i\varepsilon_{k'} t'} M(|\mathbf{k}' - \mathbf{k}|, \varepsilon_{k'} - \varepsilon_k, t''), \quad (\text{B22})$$

A_1 , A_2 , B_1 , and B_2 can be written as

$$A_1 = \gamma(R', R'', t, 0, t), \quad (\text{B23})$$

$$A_2 = \gamma(R'', R', t, 0, 0), \quad (\text{B24})$$

$$B_1 = \gamma(R', R'', 0, t, 0), \quad (\text{B25})$$

$$B_2 = \gamma(R'', R', 0, t, -t). \quad (\text{B26})$$

The correlation hole is given by

$$\rho_c(R, R', \theta; t < 0) = \frac{A_1 + A_2}{G_0(R, t < 0)}, \\ \rho_c(R, R', \theta; t > 0) = \frac{B_1 + B_2}{G_0(R, t > 0)}. \quad (\text{B27})$$

¹ R. M. Martin, *Electronic Structure: Basic Theory and Practical Methods* (Cambridge University Press, Cam-

bridge, 2004).

- ² L. Hedin, Phys. Rev. **139**, A796 (1965).
- ³ G. D. Mahan, *Many-Particle Physics* (Springer New York, NY, 2000).
- ⁴ R. M. Martin, L. Reining, and D. M. Ceperley, *Interacting Electrons: Theory and Computational Approaches* (Cambridge University Press, Cambridge, 2016).
- ⁵ F. Aryasetiawan and F. Nilsson, *Downfolding Methods in Many-Electron Theory* (AIP Publishing, Melville, New York, 2022).
- ⁶ F. Aryasetiawan and O. Gunnarsson, Rep. Prog. Phys. **61**, 237 (1998).
- ⁷ A. L Fetter and J. D Walecka, *Quantum Theory of Many-Particle Systems*, (Dover, Mineola, New York, 2003).
- ⁸ J. W. Negele and H. Orland, *Quantum Many-Particle Systems*, (Westview Press, Boulder, Colorado, 1998).
- ⁹ F. Aryasetiawan, Phys. Rev. B **105**, 075106 (2022).
- ¹⁰ F. Aryasetiawan and T. Sjöstrand, Phys. Rev. B **106**, 045123 (2022).
- ¹¹ O. Gunnarsson and B. I. Lundqvist, Phys. Rev. B **13**, (4274 1976).
- ¹² R. O. Jones and O. Gunnarsson, Rev. Mod. Phys. **61**, 689 (1989).
- ¹³ D. Pines and D. Bohm, Phys. Rev. **85**, 338 (1952).
- ¹⁴ P. Hohenberg and W. Kohn, Phys. Rev. **136**, B864 (1964).
- ¹⁵ W. Kohn and L. J. Sham, Phys. Rev. **140**, A1133 (1965).
- ¹⁶ A. D. Becke, J. Chem. Phys. **140**, 18A301 (2014).
- ¹⁷ R. O. Jones, Rev. Mod. Phys. **87**, 897 (2015).
- ¹⁸ J. C. Slater, Phys. Rev. **81**, 385 (1951).
- ¹⁹ Y. Wang and J. P. Perdew, Phys. Rev. B **44**, 13298 (1991).
- ²⁰ N. W. Ashcroft and N. D. Mermin, *Solid State Physics*, (Saunders College Publishing, NY, 1976)